© Strojniški vestnik 48(2002)5,244-256
ISSN 0039-2480
UDK 667.644.3:532.525:519.61/.64
Izvrini znanstveni članek (1.01)

© Journal of Mechanical Engineering 48(2002)5,244-256
ISSN 0039-2480
UDC 667.644.3:532.525:519.61/.64
Original scientific paper (1.01)

Tokovne razmere v avtomobilski lakirnici: numerična in eksperimentalna analiza

Flow Conditions in an Automotive Spray-Paint Chamber: Numerical and Experimental Analyses

Jure Marn - Zoran Žunič - Matjaž Ramšak - Primož Ternik

V prispevku smo analizirali tokovne razmere v avtomobilski lakirni komori. Za reševanje Navier-Stokesovih enačb prostorskega toka nestisljive izotermne tekočine smo uporabili metodo nadzornih prostornin (CFX 5.4). Podrobno smo opisali potek izračuna, uporabljene robne in začetne pogoje, uporabljene metode za stabilizacijo numeričnih nihanj ter druge parametre, pomembne za izračun. Predstavili smo rezultate za ravninski in prostorski primer izračuna. Robni pogoji so bili določeni z meritvami na realni komori in to za primer brez avtomobila in z njim. Filter komore je bil upoštevan kot porozna snov s kvadratno funkcijo upora po podatkih proizvajalca, ki smo jih preverili z lastnimi meritvami padca tlakov.

(Ključne besede: komore lakirne, dinamika tekočin, analize numerične, turbulenca)

This paper deals with the flow analysis around a car in a spray-paint chamber. To solve the Navier-Stokes equations for 3D flow of an incompressible and isothermal fluid we used the control-volume method (CFX 5.4). The numerical procedure, the boundary and initial conditions, the methods used for stabilizing the numerical oscillations as well as the other parameters important for the numerical procedure are described in detail. Results for 2D and 3D calculations are presented. The boundary conditions were determined with measurements in a real chamber with and without a car. The filter in the chamber was considered to be porous matter with a quadratic law of resistance, this is in accordance with the manufacturer's data that were verified with pressure-loss measurements.

(Keywords: spray-paint chamber, fluid dynamic, numerical analysis, turbulence)

0 UVOD IN SPODBUDA ZA DELO

V pričujočem prispevku smo se ukvarjali z analizo toka okoli avtomobila v lakirnici. Med lakiranjem je zelo pomembno, da zrak teče okoli avtomobila kar se da mirno, s čim manjšimi vrtinci, še zlasti pa se želimo izogniti recirkulacijskim conam, kjer bi zaradi pojavov vrtinčenja in zato ponovnega dviga prahu lahko prišlo do usedanja prašnih delcev na sveže pobarvane dele avtomobilske karoserije, s tem pa do napak pri lakiranju.

Analizo bi bilo moč opraviti na dva načina. Pri prvem bi se lahko naslonili na eksperimentalno analizo, pri kateri bi na določene točke v lakirnici postavili dimne vire in opazovali tirnice dimnih delcev skozi lakirnico. Težava pri takem postopku bi bila v omejeni uporabi, saj bi lahko ugotovili recirkulacijske cone le za določen tip vozila in za določene robne pogoje, in v nenatančnosti, saj bi se lahko zgodilo, da bi zgrešili kako recirkulacijsko območje. Drugi način je numerična analiza, pri kateri

0 INTRODUCTION AND MOTIVATION FOR THE WORK

In this paper we have analyzed the flow around a car in a spray-paint chamber. During the process of lacquering it is very important that the air flows around the car as smoothly as possible, generating the smallest eddies possible. However, most importantly, we wish to avoid recirculation zones, where curling and the resulting dust raising could cause the deposition of dust particles on the freshly painted car body, which eventually means a degradation of the paint quality.

An analysis could be performed in two ways. First, we could use an experimental analysis that involved mounting smoke sources at certain points in the lacquer chamber and the observing the path of the smoke particles through the lacquer chamber. The disadvantage of this approach is in its limited application: the recirculating zones can only be observed for a certain type of car and for certain boundary conditions, and there is also the uncertainty that would arise because we could overlook some recirculating

lahko robne pogoje spreminjamo, prav tako tudi geometrijsko obliko. Tak način je preprostejši, ker modeliramo večino geometrijskih parametrov le prvič, nato pa spreminjamo vstopne in izstopne pogoje ter ugotavljamo spremembe.

Poleg želje po določitvi recirkulacijskih območij smo želeli še zlasti prikazati, kako je moč primerno uporabiti sedanja orodja računalniške dinamike tekočin in hkrati eksperimentalno določiti robne pogoje. Prav ti v primeru uveljavljenih orodij, npr. CFX, katerih ovrednotenje in preveritev sta bili že opravljeni, pogosto določajo kakovost rezultatov.

0.1 Opis lakirnice

V obravnavanem primeru gre za lakirnico dolžine 5880 mm, širine 3560 mm in največje višine 2480 mm. Zrak vstopa v lakirnico s stropa in izstopa v okolico skozi talno rešetko dolžine 4000 mm in širine 3000 mm ter nato v kanal na dnu lakirnice. Kanal vodi na prosto skozi izpust zraka prizmatične oblike širine 1000 mm, višine 860 mm in pri vrhu globine 650 mm, pri čemer je izpust zavarovan z izpustno rešetko z žaluzijami. Talna rešetka je prekrita s filtri debeline 50 mm, ki barvi, razpršeni v zraku, preprečujejo izstop v okolico in onesnaženje.

Ventilator in grelnik zraka za to analizo nista bila pomembna, zato njunih tehničnih podatkov ne navajamo.

1 MERITVE

V sami lakirnici smo opravili dvoje vrst meritev, in sicer meritve zaradi določitve robnih pogojev in meritve zaradi določitev snovskih lastnosti filtra. Kakor je bilo že zapisano, je bil končni cilj zastavljene naloge numerična analiza toka okoli avtomobila v lakirnici z željo, da bi določili morebitne recirkulacijske cone. Taka numerična analiza je neprimerno hitrejša in cenejša od meritev v vseh pomembnih točkah okoli avtomobila, poleg tega pa ni nasilna, je pa po naših izkušnjah odvisna zlasti od določitve robnih in začetnih pogojev ter snovskih lastnosti.

1.1 Opis meritev robnih pogojev

V prvem delu raziskav za določitev robnih pogojev smo izvedli meritve hitrosti v osmih točkah ob stropu vstopnega dela, ki so prikazane na sliki 1.

Meritve smo opravili v dveh razporedih, brez avtomobila in z njim, pri čemer nismo pričakovali bistvenih razlik med posameznimi rezultati. Vsako od meritev smo opravili po dvakrat, da bi zmanjšali velikost napak.

Meritve smo opravili z ročnim merilnikom z vročo žičko. Merilnik smo pred izvajanjem meritev

zones. Second, we can take advantage of numerical analysis where we can modify the boundary and initial conditions as well as the geometry. This approach is simpler because we model most of the geometrical parameters only once, and then by modifying the inlet and outlet conditions we can follow the changes.

In addition to determining the recirculating zones we particularly wanted to present the use of existing numerical tools and to experimentally determine the boundary conditions. In the case of well-known programs, in our case CFX, which were validated and verified, it is the boundary conditions that suggest the results' quality.

0.1 Spray-paint chamber

The spray-paint chamber is 5,880 mm in length, 3,560 mm in width and has a maximum height of 2,480 mm. Air enters the chamber from the ceiling and exits through the floor grid which is 4,000 mm in length and 3,000 mm in width, and then flows into the channel below the chamber. The channel leads to the outside through the prismatic opening that is 1,000 mm wide, 860 mm high and 650 mm deep. The outlet is secured with a shuttered grid. The floor grid is covered with a 50-mm-thick filter that prevents the dispersed paint from polluting the environment.

The ventilator and the air heater are not important for this analysis and therefore we do not give any technical specifications for them.

1 MEASUREMENTS

In the spray-paint chamber we performed two kinds of measurements: measurements for determining the boundary conditions and measurements for determining the filter properties. As already stated, we wanted to perform a numerical simulation of the flow around a car in a spray-paint chamber and determine the recirculation zones. A numerical analysis is much faster and cheaper than measurements at all the important points around the car, and more over, it is a non-invasive procedure. We also believe that the numerical analysis plays an important role in determining the boundary and initial conditions as well as the physical properties.

1.1 Description of the boundary-conditions measurement

In the first part of our analysis we measured the velocity at eight points in the inlet region (Figure 1).

The measurements were made with and without a car. We did not expect significant differences for particular results. Each measurement was performed twice in order to reduce the magnitude of the errors.

The measurements were made with a manual hot-wire anemometer. The instrument was calibrated

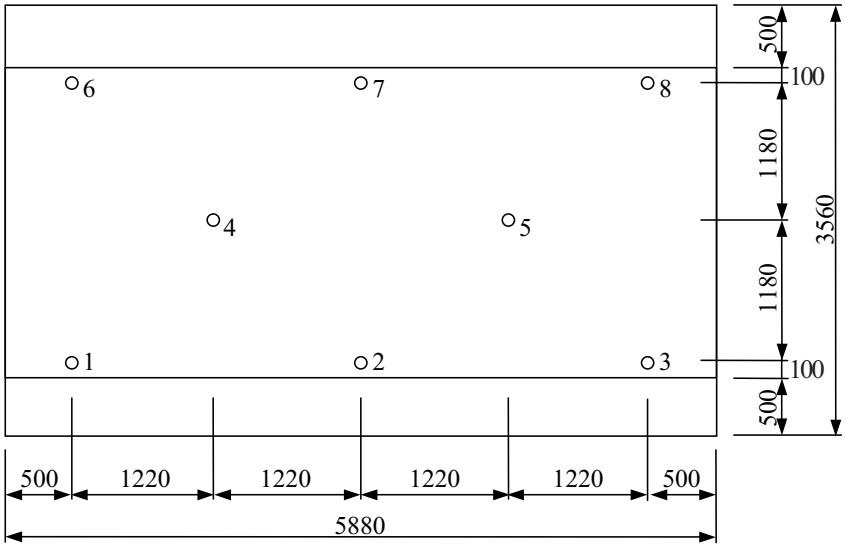

Sl. 1. *Merilne točke v lakirni komori (izmere v mm)*
Fig. 1. *Measurement points in spray-paint chamber (dimensions in mm)*

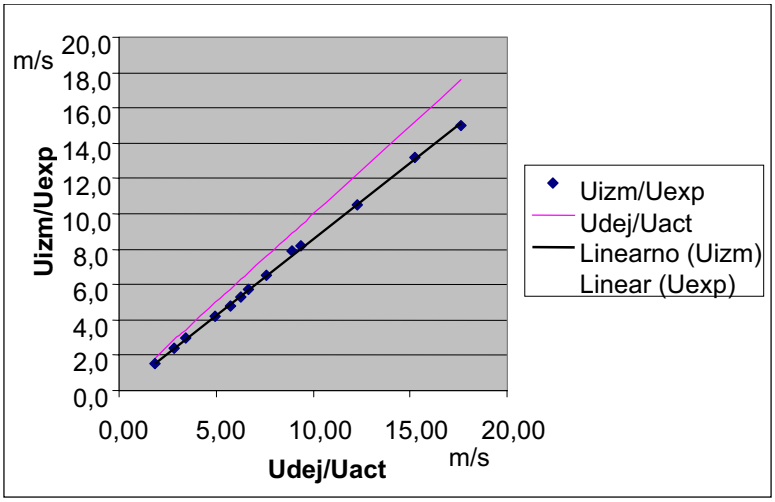

Sl. 2. *Napaka ročnega merilnika hitrosti z vročo nitko glede na primerjalno hitrost*
Fig. 2. *Error of manual hot-wire anemometer according to reference velocity*

umerili na testni progi iz plastičnih cevi premera 120 mm, v katerega smo tlačili zrak skozi cev z uporabo aksialno-radialnega ventilatorja IMP. Proga je opremljena s Pitotovo cevjo, dinamični tlak in padec tlaka pa smo izmerili z manometrom BETZ natančnosti 1 Pa. Meritve smo opravili med 2,1 m/s in 8,0 m/s ter ugotovili natančnost nitke med +1,50% in +4%. Ugotovimo lahko torej, da je v merilnem območju natančnost merilnika +4%, natančnejši rezultati pa so prikazani na sliki 2.

Opravili smo tudi meritve pri vhodu v merilno komoro in ugotovili, da je puščanje zraka iz lakirne komore zanemarljivo, vsekakor pa znotraj merilne negotovosti merilnega instrumenta. Zato smo predpostavili, da ves zrak vstopa pri vrhu in izstopa pri dnu. Prav tako smo predpostavili, da so vrednosti vstopnih hitrosti pri vrhu linearno interpolirane med posameznimi merilnimi točkami.

in a test line made of plastic pipes with a diameter of 120 mm that was fed with air by means of an IMP axial-radial ventilator. The line was equipped with a Pitot pipe, the dynamic pressure and the pressure drop were measured with a BETZ manometer of accuracy 1 Pa. The measurements were performed between 2.1 m/s and 8.0 m/s, and the determined accuracy of a hot wire is between +1.5% and +4%. We can conclude that in the selected measurement range the precision of the data is within +4%. More detailed results are presented in Figure 2.

The measurements at the inlet of the spray-paint chamber indicated that any leakage of air from the spray-paint chamber is negligible and still within the measurement uncertainty of the instrument. We supposed that the air enters at the top and leaves at the bottom. We also assumed that all the values of the inlet velocities at the top are linearly interpolated between the particular measurement points.

1.2 Opis in rezultati meritev padca tlaka skozi filter

Kakor smo že zapisali, je bila talna rešetka prekrita s filtrom debeline 50 mm. V dejanskem primeru je bil uporabljen filter KONUS KOFIL KFS 50, za katerega je proizvajalec v svoji specifikaciji podal tri merilne točke upora v odvisnosti od hitrosti zraka, ki teče skozi filter. Te podatke smo želeli laboratorijsko preveriti. Uporabljena merilna proga je bila enaka tisti, uporabljeni za umerjanje ročnega merilnika hitrosti, na slikah 3 in 4 pa so prikazani rezultati.

1.2 Description and measurements results of the pressure drop through the filter

The lattice was covered with a 50-mm-thick filter. In the real process a KONUS KOFIL KFS 50 filter was used, for which the manufacturer, in its specification, gave three points of resistance depending on the air speed flowing through the filter. These data were experimentally examined. The measurement lane was the same as the one used for calibrating the manual velocity measurer, the results are shown in Figures 3 and 4.

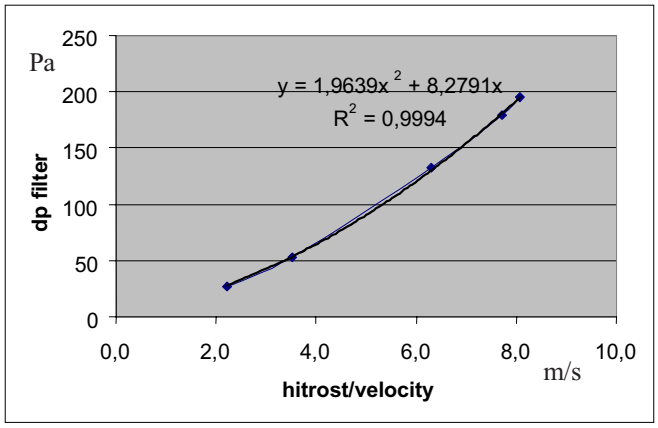

Sl. 3. *Tlačni padec skozi filter kot funkcija hitrosti zraka*
Fig. 3. *Pressure drop through filter as a function of air speed*

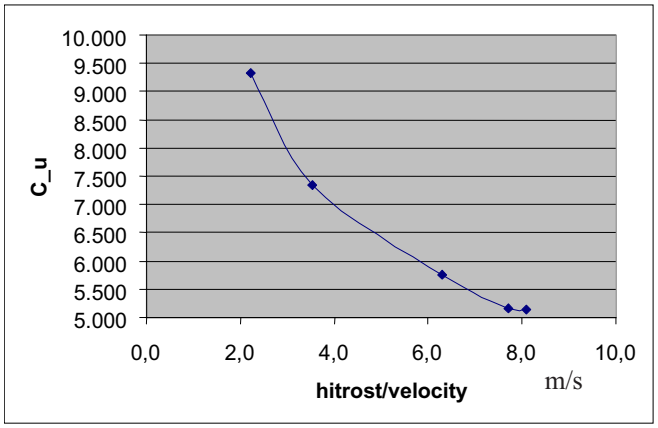

Sl. 4. *Količnik upora filtra kot funkcija hitrosti*
Fig. 4. *Resistance coefficient of filter as a function of velocity*

1.3 Rezultati meritev robnih pogojev na vstopu in izstopu

V postopku izvedbe meritev robnih pogojev na vstopu smo izvedli štiri nize preskusov brez avtomobila in dva niza preskusov z njim v vsaki od točk, da bi zmanjšali vpliv napak. Rezultati so prikazani v preglednicah 1 (brez avtomobila) in 2 (z avtomobilom). V vsaki točki je prikazano tudi odstopanje od srednje vrednosti.

Izmerili smo tudi profil hitrosti na izhodu, a smo imeli zaradi izstopnih žaluzij težave z razlago rezultatov. Lega žaluzij namreč povzroča, da tok zraka periodično

1.3 Results of the boundary conditions during inlet and outlet measurements

When measuring the boundary conditions at the inlet, four sets of experiments with the car and two sets of experiments without the car were performed. The goal was to reduce the influence of experimental errors. The results are shown in Table 1 (without the car) and Table 2 (with the car). For each experimental point the deviation about the mean is also shown.

We have also measured the velocity profiles at the outlet, but the grid shuttles caused problems with the interpretation of the results. The position of

Preglednica 1. *Hitrost zraka v m/s v posamezni merilni točki na vstopu v komoro brez avtomobila*
Table 1. *Air velocity in m/s at a particular measurement point for the chamber inlet without car*

	I	II	III	IV
1	0,32	0,35	0,32	0,35
2	0,28	0,38	0,38	0,28
3	0,40	0,38	0,35	0,40
4	0,38	0,48	0,42	0,42
5	0,28	0,25	0,28	0,30
6	0,38	0,40	0,40	0,35
7	0,40	0,32	0,35	0,40
8	0,38	0,35	0,35	0,35
Povprečje/Average	0,3525	0,3638	0,3563	0,3563
Odstopanje/Deviation	0,0444	0,0463	0,0328	0,0378

Preglednica 2. *Hitrosti zraka v m/s v posamezni merilni točki na vstopu v komoro z avtomobilom*
Table 2. *Air velocity in m/s at a particular measurement point for the chamber inlet with car*

	I	II
1	0,41	0,4
2	0,28	0,4
3	0,42	0,35
4	0,38	0,38
5	0,28	0,28
6	0,32	0,4
7	0,48	0,4
8	0,28	0,35
Povprečje/Average	0,3563	0,3700
Odstopanje/Deviation	0,0663	0,0325

spreminja hitrost, saj žaluzije tok usmerjajo in se za njimi ustvarjajo cone recirkulacije. Tako smo rezultate uporabili zgolj za oceno pravilnosti izračunanega masnega toka zraka na izstopu.

1.4 Merilna negotovost

1.4.1 Osnove za izračun merilne negotovosti

Dinamični tlak na Pitotovi cevi in padec tlaka na filtru merimo z Betzovim manometrom, katerega natančnost je ocenjena na 1Pa. Pri tem je ločljivost skale Betzovega manometra 0,1mm.

Hitrost zraka izračunamo z Bernoullijevo enačbo:

$$v = \sqrt{\frac{2 \cdot p_d}{\rho}} \qquad (1),$$

kjer je:
p_d - dinamični tlak na Pitotovi cevi,
$\rho = 1{,}164\ \mathrm{kg/m^3}$ - gostota zraka pri $T = 20°\mathrm{C}$.

Koeficient upora filtra C_u izračunamo z uporabo izraza za lokalne izgube:

$$C_u = \frac{2 \cdot \Delta p}{\rho \cdot v^2} \qquad (2),$$

kjer je:
Δp - padec tlaka na filtru.

the shuttles causes periodically changing velocities due to the influence of the shuttles on the direction of the flow. Velocity profiles were therefore only used for a verification of the mass flow through the outlet.

1.4 Measurement uncertainty

1.4.1 Basics of measurement uncertainty calculation

The dynamic pressure at the Pitot pipe and pressure drop through the filter are measured with the BETZ manometer. The scale resolution of the BETZ manometer is 0.1 mm.

The air speed is determined from Bernoulli's equation as:

$$v = \sqrt{\frac{2 \cdot p_d}{\rho}} \qquad (1),$$

where:
p_d - dynamic pressure at the Pitot pipe
$\rho = 1.164\ \mathrm{kg/m^3}$ - density of air at $T = 20°\mathrm{C}$.

The resistance coefficient C_u is determined with the equation for local pressure losses:

$$C_u = \frac{2 \cdot \Delta p}{\rho \cdot v^2} \qquad (2),$$

where:
Δp - pressure drop through the filter.

Preglednica 3. *Rezultati meritev*
Table 3. *Results of measurements*

točka point	p_d Pitot (Pa)	Δp filter (Pa)	v Pitot (m/s)	v anem (m/s)	Cu filter
1	2,94	27,41	2,25	2,30	9,33
2	7,34	53,85	3,55	3,60	7,33
3	23,50	135,11	6,35	6,40	5,75
4	35,25	182,10	7,78	8,00	5,17
5	38,67	198,74	8,15	8,40	5,14

1.4.2 Določitev merilne negotovosti

Ker je standardna merilna negotovost posredno merjene veličine:

$$u(y) = \sqrt{\sum_{i=1}^{M} \left(\frac{\partial f}{\partial x_i} \right)^2 \cdot u^2(x_i)} \tag{3}$$

lahko ob upoštevanju, da je $u(\rho) = 0$, zapišemo skupno standardno merilno negotovost hitrosti zraka:

$$u(v) = \sqrt{\left(\frac{\partial v}{p_d} \right)^2 \cdot u^2(p_d)} = \sqrt{\left(\frac{1}{2 \cdot \rho \cdot p_d} \right) \cdot u^2(p_d)} \tag{4}$$

in količnika upora:

$$u(C_u) = \sqrt{\left(\frac{\partial C_u}{\partial \Delta p} \right)^2 \cdot u^2(\Delta p) + \left(\frac{\partial C_u}{\partial v} \right)^2 \cdot u^2(v)} = \sqrt{\left(\frac{2}{\rho \cdot v^2} \right)^2 \cdot u^2(\Delta p) + \left(-\frac{4 \cdot \Delta p}{\rho \cdot v^3} \right)^2 \cdot u^2(v)} \tag{5}.$$

Ker je $u(\Delta p) = u(p_d) = u_B(p_d)$ (meritev izvedena le enkrat), sta posamezni merilni negotovosti:

$$u(v) = \sqrt{\left(\frac{1}{2 \cdot \rho \cdot p_d} \right) \cdot u_B^2(p_d)} \tag{6}$$

in

$$u(C_u) = \sqrt{\left(\frac{2}{\rho \cdot v^2} \right)^2 \cdot u_B^2(\Delta p) + \left(-\frac{4 \cdot \Delta p}{\rho \cdot v^3} \right)^2 \cdot \left(\frac{1}{2 \cdot \rho \cdot p_d} \right) \cdot u_B^2(p_d)}. \tag{7}$$

Merilno negotovost tipa B Betzovega manometra določimo z upoštevanjem njegove natančnosti (1 Pa):

$$u_B'(p_d) = u_B'(\Delta p) = \frac{1Pa}{\sqrt{3}} = 0,577Pa \tag{8}$$

in ločljivosti skale (0,1 mm oz. 0,979 Pa):

$$u_B''(p_d) = u_B''(\Delta p) = \frac{0,979Pa}{\sqrt{3}} = 0,565Pa \tag{9}$$

kot

$$u_B(p_d) = u_B(\Delta p) = \sqrt{u_B'^2(p_d) + u_B''^2(p_d)} = 0,808Pa \tag{10}.$$

Rezultati vseh merilnih točk prikazuje preglednica 4.

Merilna negotovost samih meritev, ki so bili opravljeni na progi, je enaka merilni negotovosti tipa B, ki pa se ujema z merilno negotovostjo instrumenta.

1.4.2 Measurement-uncertainty determination

Considering that the combined standard uncertainty is:

and $u(\rho) = 0$, we can write the combined standard uncertainty of the air speed as:

and the coefficient of resistance as:

Because $u(\Delta p) = u(p_d) = u_B(p_d)$, we can write:

and:

The type B component of measurement uncertainty for the BETZ manometer is determined by considering its accuracy (1 Pa):

and scale resolution (0.1 mm, corresponding to 0.979 Pa):

as:

The results for all experimental points are shown in Table 4.

The measurement uncertainty of the measurements is equal to the type B component of the measurement uncertainty, which coincides with the measurement uncertainty of the instrument.

Preglednica 4. *Merilna negotovost u(v) in u(Cu)*
Table 4. *Measurement uncertainties u(v) and u(Cu)*

točka point	v Pitot (m/s)	u(v) (m/s)	Cu filter	u(Cu)
1	2,25	0,309	9,33	2,56
2	3,55	0,195	7,33	0,81
3	6,35	0,109	5,75	0,20
4	7,78	0,089	5,17	0,12
5	8,15	0,085	5,14	0,11

2 NUMERIČNA ANALIZA

2.1 Vodilne enačbe

Reševali smo splošno znane Reynoldsove povprečene Navier-Stokesove enačbe (RANS) za prostorski tok nestisljive izotermne tekočine:

$$\frac{\partial u_j}{\partial x_j} = 0 \tag{11},$$

$$\rho \frac{\partial u_i}{\partial t} + \rho u_j \frac{\partial u_i}{\partial x_j} = -\frac{\partial p}{\partial x_i} + \frac{\partial}{\partial x_i}\left[\mu \left(\frac{\partial u_i}{\partial x_j} + \frac{\partial u_j}{\partial x_i} \right) - \rho \overline{u_i' u_j'} \right] \tag{12},$$

kjer je u časovno povprečeni hitrostni vektor, x krajevni vektor, p časovno povprečeni tlak, ρ gostota, μ dinamična viskoznost in zadnji člen na desni strani enačbe zveza med hitrostnimi nihanji, ki jo imenujemo tudi Reynoldsov napetostni tenzor.

Za modeliranje Reynoldsovega napetostnega tenzorja uporabimo dvoenačbni model k-ε:

$$-\rho \overline{u_i' u_j'} = \mu_T \left(\frac{\partial u_i}{\partial x_j} + \frac{\partial u_j}{\partial x_i} \right) - \frac{2}{3} \rho \; k \delta_{ij} \tag{13},$$

$$\mu_T = c_\mu \rho \frac{k^2}{\varepsilon} \tag{14},$$

kjer je μ_T dinamična turbulentna viskoznost, k turbulentna kinetična energija, ε stopnja turbulentnega raztrosa, δ_{ij} Kroneckerjeva delta funkcija in c_m empirična konstanta z vrednostjo 0,09.

Za modeliranje izotropnega upora tekočine uporabimo kvadratni zakon upora. Izvirni člen S_M v gibalni enačbi se glasi:

$$S_i = -C_{R1} u_i - C_{R2} |u_i| \; u_i \tag{15},$$

kjer sta C_{R1} in C_{R2} koeficienta upora.

Zraven enačb (11) in (12) dobimo še dve prenosni enačbi za k in ε:

$$\rho \frac{\partial k}{\partial t} + \rho u_j \frac{\partial k}{\partial x_j} = \frac{\partial}{\partial x_j}\left(\mu + \frac{\mu_T}{\sigma_k} \frac{\partial k}{\partial x_j} \right) + P - \rho \varepsilon \tag{16},$$

$$\rho \frac{\partial \varepsilon}{\partial t} + \rho u_j \frac{\partial \varepsilon}{\partial x_j} = \frac{\partial}{\partial x_j}\left(\mu + \frac{\mu_T}{\sigma_\varepsilon} \frac{\partial \varepsilon}{\partial x_j} \right) + c_1 \frac{\varepsilon}{k} P - c_2 \rho \frac{\varepsilon^2}{k} \tag{17},$$

kjer sta σ_k in σ_ε turbulentni Prandtlovi števili za k in ε, c_1 in c_2 pa sta empirični konstanti. V našem primeru so imele konstante vrednost σ_k=1,0; σ_ε=1,3; c_1=1,44 in c_2=1,92.

2 NUMERICAL ANALYSIS

2.1 Leading equations

We were solving the generally known Reynolds' averaged Navier-Stokes equations (RANS) for the 3D flow of incompressible and isothermal flow:

(11), (12),

where u a is time-averaged velocity vector, x is a spatial vector, p is the time-averaged pressure, ρ is the density, μ is the dynamic viscosity and the last term on the right-hand side of the equation is the correlation between the velocity fluctuations, also known as the Reynolds stress tensor.

The Reynolds stress tensor is modeled with a two-equation k-ε model

(13), (14),

where μ_T is the dynamic turbulent viscosity, k is the turbulent kinetic energy, ε is the level of turbulent dissipation, δ_{ij} is Kronecker's delta function and c_m is the empirical constant with a value of 0.09.

The isotropic resistance of the fluid was modeled with the quadratic law of resistance. The source term S_M in the equation of motion is:

(15),

where C_{R1} and C_{R2} are resistance coefficients.

Besides equations (11) and (12) we obtain two transport equations for k and ε:

(16), (17),

where σ_k and σ_ε are turbulent Prandtl's numbers for k and ε, and c_1 and c_2 are empirical constants. In our case the values for the constants were σ_k=1.0, σ_ε=1.3, c_1=1.44 and c_2=1.92.

Člen P imenujemo produkcija in je definiran kot:

$$P = \mu_T \left(\frac{\partial u_i}{\partial x_j} + \frac{\partial u_j}{\partial x_i} \right) \frac{\partial u_i}{\partial x_j} \quad (18).$$

2.2 Postopek reševanja

Zgoraj opisane enačbe so bile po postopku nadzornih prostornin spremenjene v sistem algebrajskih enačb.

Sisteme linearnih enačb smo reševali na delno povezan način, kar pomeni, da so bile v eni iteraciji reševane kontinuitetna in tri gibalne enačbe, nato pa še ločeno enačbi za turbulentno kinetično energijo in turbulentnim raztrosom. Na tak način dosežemo kompromis med številom nelinearnih iteracij in potrebno količino pomnilnika za rešitev sistema enačb.

Za reševanje sistemov linearnih enačb smo uporabili algebrsko večmrežje z dodano popravo. Tako najbolje izkoristimo dejstvo, da diskretizirane enačbe pomenijo ohranitev bilance osnovnih spremenljivk v nadzorni prostornini. Enačbe redke mreže dobimo preprosto z združevanjem posameznih prostornin goste mreže. Z numeričnega vidika je večmrežje učinkovitejše kakor druge metode. Na dani mreži so lahko iterativni rešilniki učinkoviti le pri zmanjševanju napak, ki imajo valovne dolžine velikosti mreže. Slabše se obnesejo pri napakah z valovnimi dolžinami velikostnega reda računskega območja. Metoda večmrežja obide navedeno težavo z navideznim redčenjem osnovne mreže v postopku iterativnega reševanja sistema enačb, reševanjem enačbe za popravo na redki mreži in nato podaljšanje poprave nazaj na fino mrežo. Redka mreža je zmožna gladiti napake nižjih frekvenc kot fina mreža, tako da z nekaj nivoji redčenja osnovne mreže pokrijemo celoten frekvenčni spekter napak, kar ima za posledico boljšo konvergenco.

Za stabilizacijo konvektivnega člena smo uporabili protivetrno metodo prvega reda natančnosti. Zanjo smo se odločili predvsem zaradi njene numerične stabilnosti. Mogoče bi bilo uporabiti tudi višjeredno metodo popravek numerične korekcije, ki pa je zaradi možnega pojava numerične disperzije in večje porabe računalniškega časa nismo uporabili.

Viskozni podsloj, ki nastane ob steni pri turbulentnem toku modeliramo z uporabo posebnih zidnih elementov. V zidnih elementih uporabimo oblikovne funkcije, ki so posebej prirejene, da zajamejo strme spremembe osnovnih spremenljivk v viskoznem podsloju. Te funkcije temeljijo na splošnem "zidnem zakonu" in so odvisne od karakterističnih turbulentnih Reynoldsovih števil. Med iterativnim postopkom reševanja se spreminjajo, da bi čim bolje zajele lokalne razmere.

The term P is called production and is defined as:

2.2 Solving procedure

The above equations were transformed into a system of algebraic equations following the procedure of the control-volume method.

The systems of linear equations were solved in a partially coupled manner. In one iteration the continuity equation and three momentum equations were solved coupled, followed by the equations for turbulent kinetic energy and turbulent dissipation. This is the compromise between the number nonlinear iterations and the amount of computer memory required for solving a system of equations.

The selected system of linear equations was solved using the additive-correction algebraic multigrid method. This approach takes advantage of the fact that the discrete equations are representative of the balance of conserved quantities over a control volume. The coarse-mesh equations can be created by merging the original control volumes to create larger ones. From a numerical standpoint the multigrid approach offers a significant advantage. For a given mesh size, iterative solvers are only efficient at reducing errors that have a wavelength of the order of the mesh spacing. So, while shorter-wavelength errors disappear quite quickly, errors with longer wavelengths can take a very long time to disappear. The multigrid method bypasses this problem by coarsening the virtual mesh spacing during the course of the iterations, solving the equation for the coarse-mesh correction and then prolonging of the correction back to the finer mesh. The coarse-mesh smooths errors with lower frequencies, so with a few levels of coarsening we cover the whole range of error frequencies, which leads to a better convergence.

For stabilization of the convective term we used the upwind method of the first order of accuracy. The main reason for its application was its numerical stability and robustness. It could be possible to use the high-order NAC (numerical advection correction) method but we did not use it because of possible numerical dispersion.

The viscous sublayer that occurs near the wall when the flow is turbulent is modelled by using particular wall elements. In the wall elements we use shape functions that are arranged for the capture of the high primitive variables gradients in the viscous sublayer. These functions are based on a general law-of-the-wall and depend on characteristic turbulent Reynolds numbers. During an iterative procedure they change in order to better capture the local conditions.

Talni filter smo modelirali kot porozno snov s kvadratnim zakonom upora, pri čemer smo konstante modela določili po podatkih proizvajalca filtra.

2.3 Rezultati

2.3.1 Ravninski primer

V primeru ravninskega izračuna smo uporabili 72 846 elementov. Velikost elementov je znašala med 50 in 100 mm. Dobili smo sistem linearnih enačb z 19 872 neznankami. Za reševanje je bilo potrebno 49 MB (MB = 1024×1024 byte) pomnilnika.

Na vstopu smo predpisali vstopno hitrost. To hitrost smo predpisali kot povprečno vrednost v vseh merjenih točkah. Predpisali smo tudi privzete vrednosti turbulentne intenzivnosti ter mešalne dolžine (CFX 5.4). Na izstopu smo predpisali statični tlak. Predpisana natančnost reševanja je znašala 10^{-6} (kvadratna norma ostankov). Rešitev smo dobili po 90 iteracijah, za kar smo porabili 4383 s (73 min 3 s) procesorskega časa na delovni postaji Hewlett-Packard B1000. Na sliki 5 je prikazano diskretizirano območje.

The floor grid with the filter has been modelled as a porous region with the quadratic law of resistance, with the constants calculated using the filter manufacturer's data.

2.3 Results

2.3.1 2D problem

In the 2D calculation 72846 we used elements. The size of each element was between 50 and 100 mm. We were solving a system of linear equations with 19872 unknowns and we used 49 MB (MB=1024×1024 byte) of memory.

At the inlet the inlet velocity was prescribed. We prescribed it as an average value in all the points as discussed above. We also prescribed assumed values for the turbulent intensity and the mixed length (CFX 5.4). At the outlet the static pressure was prescribed. The prescribed numerical accuracy was 10^{-6} (root mean square of residuums). The solution was obtained after 90 iterations and it took 4383 s (73 min 3 s) of processor time on a Hewlett-Packard B1000 work station. Figure 5 shows the discretised area.

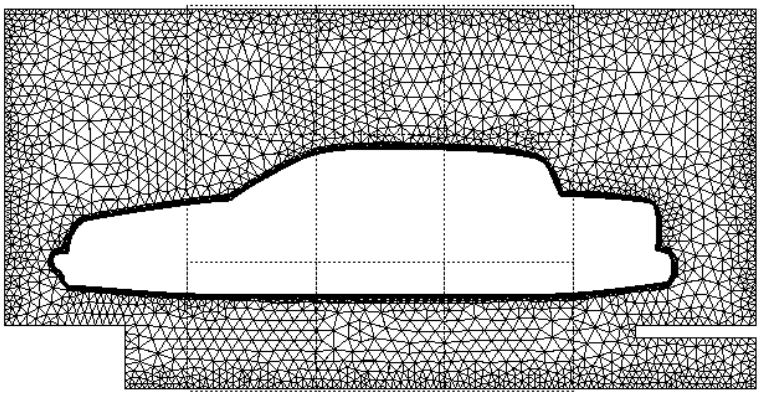

Sl. 5. *Diskretizirano območje*
Fig. 5. *Discretised area*

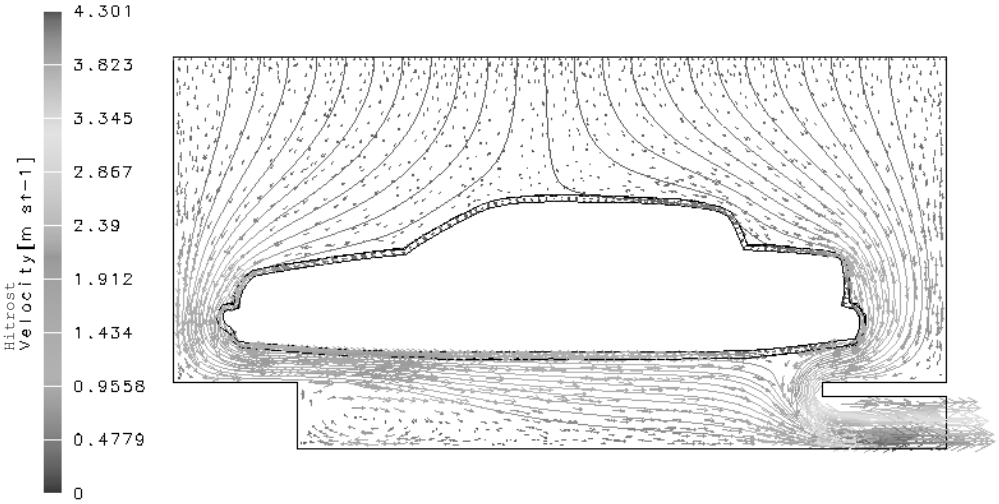

Sl. 6. *Hitrostno polje s tokovnicami*
Fig. 6. *Velocity field with stream lines*

Na sliki 6 je prikazan ravninski model avtomobila s prikazanimi vektorji hitrostnega polja in vrisanimi tokovnicami. Vidimo, da v tem, dvoizmernem primeru ne prihaja do recirkulacijskih območij v okolici avtomobila.

Na sliki 7 je prikazano polje turbulentne kinetične energije. Vidimo, da je stopnja kinetične energije v območju barvanja dokaj majhna, močno pa se poveča v izstopnem kanalu.

2.3.2 Prostorski primer

Na sliki 8 je prikazano diskretizirano območje z vrisanimi ploskovnimi elementi.

Za primere z avtomobili velikosti od 320 cm do 400 cm smo diskretizirali območje s 369620 do 355092 elementi (četverci). Velikost elementov je znašala 80 do 100 mm po površini avtomobila in komore ter 200 mm po območju. Razmerje velikosti med dvema sosednjima elementoma je bilo omejeno na 1.1. Mejno plast smo diskretizirali s tremi plastmi prizmatskih elementov. Za reševanje je bilo potrebno 190 MB pomnilnika.

Figure 6 shows the 2D model of a car with the velocity field vectors and stream lines. It can be seen that for the 2D case there are no recirculating zones.

Figure 7 shows the turbulent kinetic energy field. It can be seen that for the area of the painting it is relatively low but increases significantly in the outlet channel.

2.3.2 3D problem

Figure 8 shows the discretised area with the surface elements.

For cars with lengths between 320 cm and 400 cm the area was discretised with 369620–355092 elements (tetrahedrons). The size of the elements was set to 80–100 mm on the car body and the chamber walls' surface and 200 mm in the domain. The ratio of the size of the neighboring elements was limited to 1.1. The boundary layer was discretised with three layers of prismatic elements. For the solution of the problem 190 MB of computer memory was needed.

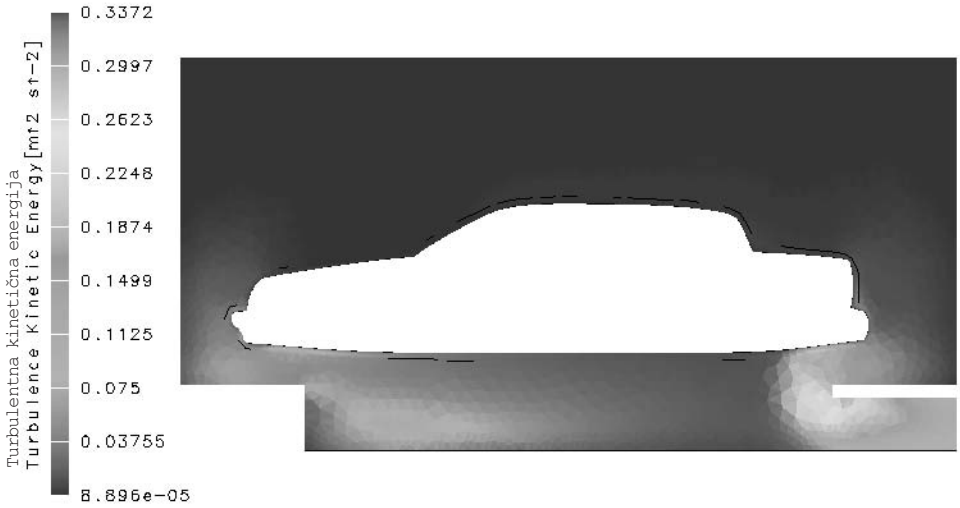

Sl. 7. *Turbulentna kinetična energija*
Fig. 7. *Turbulent kinetic energy*

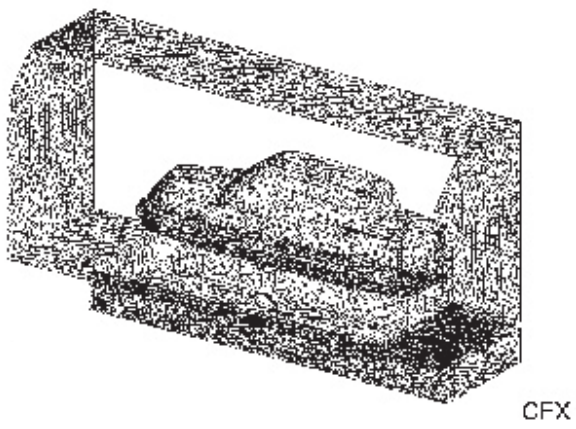

Sl. 8. *Diskretizirano območje prostorskega primera*
Fig. 8. *Discretised area of 3D example*

Na vstopu smo predpisali vstopno hitrost in privzete vrednosti turbulentne intenzivnosti ter mešalne dolžine (CFX 5.4). Na izstopu smo predpisali statični tlak. Zaradi simetričnosti območja smo modelirali samo polovico območja, na simetrijski ploskvi pa smo predpisali simetrijske robne pogoje. Kot začetne pogoje smo predpisali stanje mirovanja v območju ($v_x=v_y=v_z=0$). Predpisana natančnost reševanja je znašala 10^{-4} (kvadratna norma ostankov).

Rešitev smo dobili po 40 iteracijah, za kar smo porabili 7255 s (120 min 55 s) procesorskega časa na delovni postaji Hewlett-Packard B1000.

Na sliki 9 je prikazano hitrostno polje na simetrijski ploskvi in tlačno polje na površini avtomobila.

At the inlet the constant velocity and the default values of the turbulent intensity and the mixing length were prescribed (CFX 5.4). At the outlet the zero static pressure was prescribed. Due to the symmetrical domain only half of the chamber was discretised and symmetrical boundary conditions were prescribed. The initial condition was a zero velocity field ($v_x=v_y=v_z=0$). The prescribed convergence criterion was 10^{-4} (root mean square of residua).

The solution was obtained after 40 iterations and 7255 s (120 min 55 s) of CPU time on a Hewlett-Packard B1000 workstation.

Figure 9 shows the velocity field on a symmetry plane and the pressure field on the car-body surface.

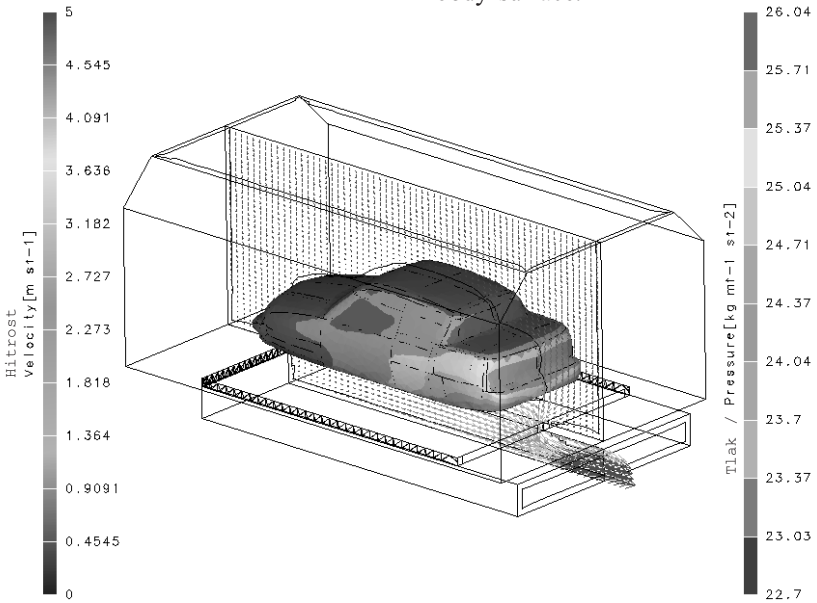

Sl. 9. *Hitrostno polje na simetrali in tlačno polje na površini avtomobila*
Fig. 9. *Velocity field on symmetry line and pressure field on a car*

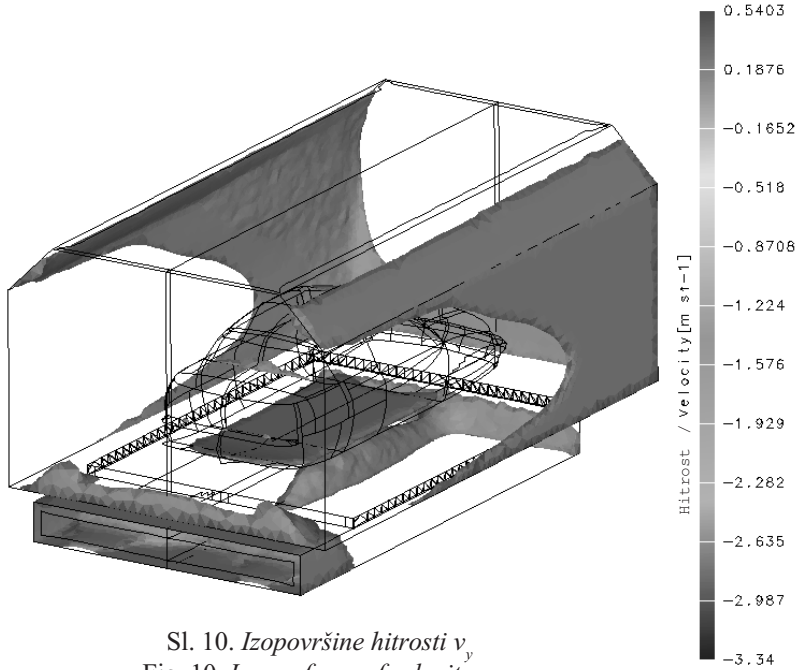

Sl. 10. *Izopovršine hitrosti* v_y
Fig. 10. *Iso-surfaces of velocity* v_y

Na sliki 10 so prikazane izopovršine hitrosti v_y, ki najbolj nazorno pokaže območja, kjer prihaja do povratnega toka (recirkulacij). Vidimo, da v okolici avtomobila ni večjih recirkulacijskih con. Po pričakovanju nastajajo manjši vrtinci v bližini sten in vogalov, kar pa na učinkovitost odvajanja barve v bližini avtomobilov ne vpliva.

Na sliki 11 so prikazane izopovršine turbulentne kinetične energije *k*, ki pove, kje so območja najbolj intenzivnega mešanja toka.

Figure 10 shows the isosurfaces of velocity v_y, which is the most illustrative way of showing zones with a recirculating flow. It can be seen that near the car-body surface no large recirculation zones exist. There are small eddies near the wall bottoms and corners as expected, but this does not have any influence on the efficiency of the painting fog removal.

Figure 11 shows the isosurface of turbulent kinetic energy *k*, which marks the areas of the most intensely mixed flow.

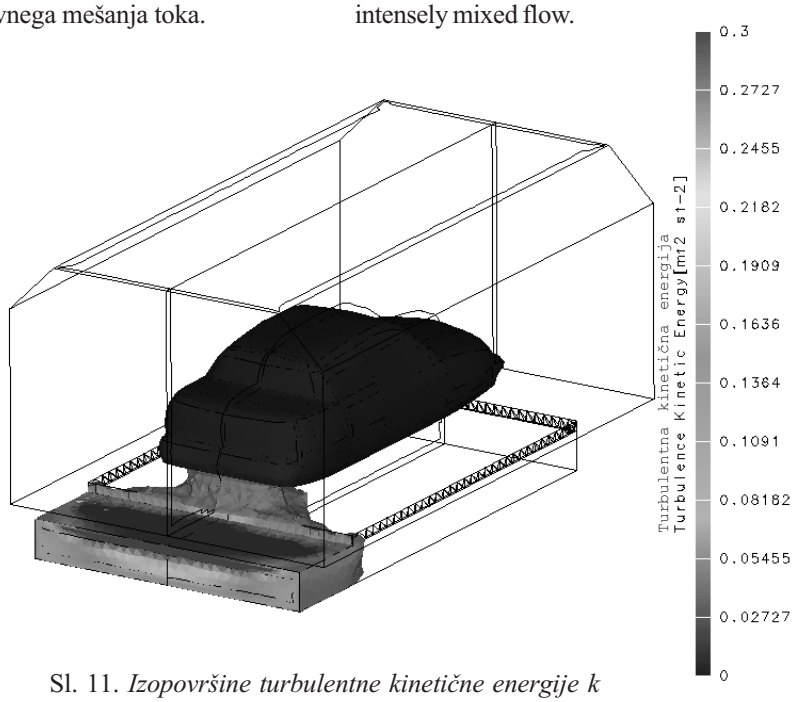

Sl. 11. *Izopovršine turbulentne kinetične energije k*
Fig. 11. *Iso-surfaces of turbulent kinetic energy k*

3 SKLEP

V prikazanem prispevku smo želeli povezati konkretno inženirsko vprašanje z metodološkim postopkom, ki omogoča preprosto spreminjanje vhodnih podatkov ter tako izdelavo variantnih rešitev brez večkratnega merjenja.

Najprej smo postavili računalniški triizmerni model lakirnice, v kateri smo želeli oceniti vpliv tokovnega polja na hrapavost nanesene barve, pri čemer smo hrapavost povezali z možnostjo recirkulacije zračnega toka. Predpostavka je nekoliko konzervativna, saj ni nujno, da vsaka recirkulacija povzroči nanos prašnih delcev, na drugi strani pa je malo verjetno, da bi prašni delci v odsotnosti recirkulacije s pomočjo difuzije napredovali proti toku zraka.

Robne pogoje smo postavili z meritvami. Izračune smo opravili z uporabo računalniškega paketa CFX in ugotovili, da v bližini realnega modela avtomobila recirkulacijskih con ni najti, kar ob upoštevanju prejšnje predpostavke pomeni, da od tega hrapavosti na lakiranih mestih avtomobila ni pričakovati.

Bistven dosežek prikazanega dela ni v končnem rezultatu in odgovoru na vprašanje glede

3 CONCLUSION

This paper deals with an engineering question and the answer based on a methodology involving a simple change of inlet parameters that gives an easy parametric analysis without repeated experiments.

First, a 3D computer model of a spray-paint chamber was built aiming to assess the influence of the fluid field on smoothness of the painted surface or better paint thereof whereas the coarseness of the painted surface was connected to recirculation of air flow. This is arguably a conservative assumption as the recirculation itself does not necessarily mean the deposition of dust particles on the painted surface.

The boundary conditions were set using measurements. The calculations were conducted using the CFX computer code and the results show that no recirculation zones were found, which means that the air flow around the vehicle should not cause the deposition of dust particles on the surface of the painted surfaces.

In itself, the final result was not the goal of this paper. The main task, i.e. showing that engineering

hrapavosti lakiranih mest na vozilu, temveč odgovor na vprašanje, da je tudi za inženirske analize in vprašanja moč uporabiti računalniško tehnologijo brez nepotrebnih poenostavitev ob uporabi meritev samo za natančno določitev robnih pogojev.

questions can be answered without undue simplification taking advantage of computer technology and relying on measurements only for as-realistic boundary conditions as possible, was in our opinion successfully achieved.

4 LITERATURA
4 REFERENCES

[1] CFX 5.4 Users manual (1999) *AEA Technology*.
[2] KOFIL, Prostorska filtracija, prospekt *Konus Konex d.o.o.*
[3] Ramšak, M., P. Ternik, J. Marn (2000) Meritev tlačnega padca za filter KONUS KOFIL KFS 50, Poročilo, Laboratorij za prenosne pojave v trdninah in tekočinah, *Fakulteta za strojništvo, Univerza v Mariboru*.
[4] Žunič, Z. (1997) Numerična obravnava problema aerodinamike vozil, Magistrsko delo, *Fakulteta za strojništvo, Univerza v Mariboru.*

Naslov avtorjev: prof.dr. Jure Marn
mag. Zoran Žunič
mag. Matjaž Ramšak
mag. Primož Ternik
Fakulteta za strojništvo
Univerze v Mariboru
Smetanova 17
2000 Maribor
jure.marn@uni-mb.si
zoran.zunic@uni-mb.si
matjaz.ramsak@uni-mb.si
primoz.ternik@uni-mb.si

Authors' Address: Prof.Dr. Jure Marn
Mag. Zoran Žunič
Mag. Matjaž Ramšak
Mag. Primož Ternik
Faculty of Mechanical Eng.
University of Maribor
Smetanova 17
2000 Maribor, Slovenia
jure.marn@uni-mb.si
zoran.zunic@uni-mb.si
matjaz.ramsak@uni-mb.si
primoz.ternik@uni-mb.si

Prejeto: 23.1.2002
Received:

Sprejeto: 23.5.2002
Accepted: